
Fractal Dimensions and Spectra of Interfaces with Application to Turbulence

Author(s): J. C. Vassilicos and J. C. R. Hunt

Source: *Proceedings: Mathematical and Physical Sciences*, Vol. 435, No. 1895 (Dec. 9, 1991), pp. 505-534

Published by: The Royal Society

Stable URL: <http://www.jstor.org/stable/52089>

Accessed: 16/10/2009 11:48

Your use of the JSTOR archive indicates your acceptance of JSTOR's Terms and Conditions of Use, available at <http://www.jstor.org/page/info/about/policies/terms.jsp>. JSTOR's Terms and Conditions of Use provides, in part, that unless you have obtained prior permission, you may not download an entire issue of a journal or multiple copies of articles, and you may use content in the JSTOR archive only for your personal, non-commercial use.

Please contact the publisher regarding any further use of this work. Publisher contact information may be obtained at <http://www.jstor.org/action/showPublisher?publisherCode=rsl>.

Each copy of any part of a JSTOR transmission must contain the same copyright notice that appears on the screen or printed page of such transmission.

JSTOR is a not-for-profit service that helps scholars, researchers, and students discover, use, and build upon a wide range of content in a trusted digital archive. We use information technology and tools to increase productivity and facilitate new forms of scholarship. For more information about JSTOR, please contact support@jstor.org.



The Royal Society is collaborating with JSTOR to digitize, preserve and extend access to *Proceedings: Mathematical and Physical Sciences*.

Fractal dimensions and spectra of interfaces with application to turbulence

BY J. C. VASSILICOS AND J. C. R. HUNT

Department of Applied Mathematics and Theoretical Physics, University of Cambridge, Silver Street, Cambridge CB3 9EW, U.K.

This paper is concerned with the analysis of any convoluted surface in two or three dimensions which has a self-similar structure, and which may simply be defined as a mathematical surface or as an interface where there is a sharp change in the value of a scalar field $F(\mathbf{x})$ (say from 0 to 1). The different methods of analysis that are related to each other here are based on spectra of the scalar which have the form

$$\Gamma(k) \propto k^{-p}, \quad (1)$$

the Kolmogorov capacity D_K of the interface or D'_K of the intersections of the interface with a plane or a line (both being defined by algorithms for counting the minimum number of boxes of sizes ϵ either covering the surface or its intersection), and the Hausdorff dimensions D_H , D'_H (which are defined differently).

It is demonstrated that interfaces with a localized self-similar structure around accumulation points, such as spirals, may have non-integer capacities D_K and D'_K even though their Hausdorff dimension is integer and equal to the topological dimension of the surface. It is explained how the same surface can have different values of D_K and D'_K over different asymptotic ranges of ϵ . There are other (fractal) surfaces where both D_H and D_K are non-integer which are convoluted on a wide range of scales with the same form of self-similarity everywhere on the surface. Distinctions are drawn between these two kinds of interface which have local and global self-similarity respectively.

If the intersections of the interface with any line form a set of points that is statistically homogeneous and independent of the location and orientation of the line and also that is self-similar over a sufficiently wide range of spacing that a capacity D'_K can be defined, it is shown that the scalar F has a power spectrum of the form of (1) and that the exponent p is related to D'_K by

$$p + D'_K = 2. \quad (2)$$

This quite general result for interfaces is verified analytically and computationally for spirals. In experiments with scalar interfaces in different turbulent flows at high Reynolds and Prandtl number, K. R. Sreenivasan, R. Ramshankar and C. Meneveau's measurements showed that $D'_K = 0.33$ for values of ϵ within the inertial range and $D'_K = 0$ for smaller values (in the microscale range). The values of p derived from (2) are consistent with the theory of G. K. Batchelor and many measurements of scalar spectra.

For fractal interfaces with global self-similarity, the values of D_H of an interface and D'_H of the intersections of the interface with a line, have been shown previously

to be related simply to each other by the topological dimension E of the interface so that $D_H = D'_H + E$. No such theorem exists in general for the Kolmogorov capacities D_K and D'_K . But it is shown analytically and computationally that for the case of spirals, over a certain range of resolutions ϵ ,

$$D_K = D'_K + E. \quad (3)$$

This corresponds in practice to the measurable range of typical experimental spirals with fewer than about five turns. Over a range of smaller length scales ϵ , where a larger number of turns is resolved and which is experimentally difficult to measure, (3) is not correct. The result (3) has been previously suggested based on experimental results.

Finally we demonstrate that interfaces for which there is a well-defined value of capacity (which is indeed the case for spirals of three turns) are only found to have self-similar spectra if there is a much wider range of length scales (e.g. more than 50 turns of the spiral) than is needed for the capacity D_K to be measurable. As well as demonstrating this computationally, this is proved mathematically for interfaces having a particular class of accumulation points whose intersections with straight lines form a self-similar sequence of points $x_n \propto n^{-\alpha}$; the power spectrum of F only tends to the self-similar form (1) if $(\epsilon_{\min}/\epsilon_{\max})^{1-D_K} \ll 1$, whereas the capacity measure simply requires that $\epsilon_{\min}/\epsilon_{\max} \ll 1$. So when $D'_K > 0$, the criteria for the spectra requires a wider range of scales in the convolutions of the interface.

This is consistent with the finding that reliable measurements of D_K can be computed from measurements of interfaces in laboratory experiments, but in the same experiments computations of spectra are often not of the form (1). Therefore, despite this apparent discrepancy with the general result (2) (which implies a value of p given a value of D'_K), the above theoretical argument supports the deduction from such experiments that if a non-integer value of D_K is measured, the interface does indeed have a self-similar structure; but it is not self-similar over a wide enough range of length scales to satisfy (2).

Consequently, for turbulent flows, stating that the capacity should have its asymptotic value rather than (as is usual) the spectrum should be equal to its asymptotic form (e.g. in (1) $p = \frac{5}{3}$) may be the correct necessary condition for deciding whether, in a given flow, the interfaces have the characteristic structure found at very high Reynolds number.

Many of the results here may be of value in other scientific fields, where convoluted interfaces are also studied.

1. Introduction

In many different kinds of flows, there are thin regions with large gradients of fluid properties across them, so that finite changes in these properties are found across these regions. A few examples of such properties are concentration, temperature, density and vorticity. These regions can usually be defined mathematically as surfaces of small but finite thickness that either move with the fluid, or that move relative to the flow as well as with the fluid (e.g. flamelets). Provided the region is thin enough compared with the smallest length scale of the flow, these surfaces can be analysed using the mathematical notion of an infinitesimally thin interface. Such situations occur in the mixing of chemically reactive substances before these

substances have had time to react, and in premixed combustion where flame fronts in the flamelet régime appear as sharp interfaces between the burned and the unburned fuel.

For an understanding of the properties of interfaces and their movement in fluid flows it is necessary to know about the geometrical structure of their deformations and foldings. Of particular interest are questions relating to the growth of the area of the interface, its space-fillingness, its stretching and its curvature. Once these properties are known, by further analysis which is specific to each particular kind of interface, it is possible to understand and model many of the processes occurring within interfaces of small but finite thickness. Where there are changes in velocity across the interface, these internal processes in part determine the movement of the interface, so the two calculations are dependent on each other and cannot be performed sequentially.

In many fluid flow problems the geometry of the interface is self-similar on different length scales, so that scaling arguments can be used as usual to indicate how experiments can be scaled up, but also to explore the space-fillingness of the interface and its invariant properties. Many of the new results and explanations presented here could be applied to many other fields in science concerned with random interfaces.

A surface can fill the space in various ways; either by accumulating around a particular point or line, as spiral shapes do, or for example, by being folded up. Actually, space-fillingness is generally understood as a property that 'fractal' surfaces have, which suggests that we should investigate how irregular the interface is, and how the above two ways of filling the space may or may not occur over a large range of scales. The problem has even deeper mathematical aspects than that, as we are really confronted with the question of how to define and give a measure for those processes, and then how to interpret that measure.

The usual methods of analysing a passive random scalar F by means of its spectrum and autocorrelation function does not appear to discriminate between different patterns or the flow fields that form them, and if they do, it is not clear how to interpret spectra in terms of the above processes. An important feature of random fields that occur in turbulent flows at high Reynolds number is their intermittency, i.e. they have very high gradients in thin regions that are well spaced out (see, for example, Frisch & Orszag 1990). Fourier methods give little information about this property of the random fields; so other methods have to be considered.

In this paper we concentrate on scalars F that are discontinuous through the interface. Batchelor (1952) has shown that there is an exponential increase of the area of isoscalar surfaces, and therefore of their increased foldings and local contortions. This property is also the cause of a cascade of increasingly small-scaled irregularities of the scalar field F , which in the case where F is constant on both sides of the interface and discontinuous through it, are irregularities or wrinkles of that interface. In practice the scales become so small that they are cut-off by physical mechanisms such as molecular diffusion, chemical reaction or flame propagation.

It is generally assumed that the self-similar cascade of eddies induces a cascade of deformations on the interface that is also self-similar (see, for example, Sreenivasan & Meneveau 1986). In fact, because small-scale turbulence is intermittent and has a power law spectrum that is non-integer, it is often assumed that turbulent interfaces become fractal, and that there are simple relations between the fractal properties of the turbulence and the surface.

Recent research indicates that by using the technique of fractals, certain

properties relating to the self-similarity and the space fillingness of interfaces can be studied in more detail than by the traditional method of spectra and autocorrelations. The main aim of this paper is to review the literature and then develop a new analysis that connects between fractal methods and spectra. In some cases this will help define more precisely the use of fractals.

2. A selective review of the literature

In random fluid motion, smooth spectra $E(k)$ that have a ‘power-law’ variation with wavenumbers (i.e. $E(k) \approx k^{-n}$) occur in a variety of cases. The most famous is the $-\frac{5}{3}$ Kolmogorov law for the inertial range of the velocity spectrum in fully developed turbulence (Batchelor 1953). Other such spectra are the k^{-2} spectrum of the solutions of Burger’s equation (Saffman 1968), the spectrum of two-dimensional turbulence (Kraichnan & Montgomery 1980), the small-scale spectrum of a temperature field passively advected by turbulence (Batchelor 1959; Batchelor *et al.* 1959), and the spectra of surface waves (Phillips 1985) and other interfaces such as occur in combustion.

Moffatt (1984) showed how a power shaped spectrum of a velocity field could be related to the structure or the topology of that velocity field. He pointed out that if the velocity field has spiral singularities or regions where sharp fluctuations or discontinuities accumulate, then the exponent of the power-shaped energy spectrum can be a non-integer and is a function of the particular nature of that ‘accumulation’ pattern. This result was obtained from a simple study of the Fourier series of a square wave (see figure 1*b*), i.e. a function that can only take one of two values, 0 or 1, over the whole space. The sharp discontinuities from 1 to 0 or from 0 to 1 of such profiles could represent the sharp jumps in any field (such as the velocity or the vorticity field). Moffatt’s result is a general result of Fourier analysis and is valid for any square shaped signal, e.g. temperature, magnetic field, pollutant concentration, etc. But it only demonstrates the existence of a relation between the exponent of the spectrum of a square shaped signal and a particular accumulation pattern of that signal. The general features are not given, and a suitable measure of the accumulation properties of the signal is not given either.

Rather than starting from spectra, an alternative approach to the analysis of random functions and random interfaces is to study their self-similarity on different length scales; or their ‘fractal’ property. As well as popularizing fractals (Mandelbrot 1982), Mandelbrot focused attention to the fact that these geometrical curiosities having fractional Hausdorff dimensions and invented by pure mathematicians in the beginning of our century (Hausdorff 1919) can actually be found in nature under various forms and in great profusion. Examples are coastlines, landscapes, trees, clouds, percolation clusters, galaxies, viscous fingers, interfaces or flamelets in turbulent flows, etc. More abstract mathematical objects having fractal properties would be brownian motions and chaotic attractors. In a series of papers in the mid and late 1970s he suggested how these ideas might be applied to the analysis of turbulent flows; in particular he attempted a study of the fractal geometry of isoscalar surfaces in turbulent velocity fields (Mandelbrot 1975) and a study of intermittency (Mandelbrot 1974).

The first experimental measure of a fractal dimension in the context of turbulence was done by Lovejoy (1982). He measured the fractal dimension D of the projection on a photographic plate of the outline of clouds and obtained 2.35. Surprisingly the

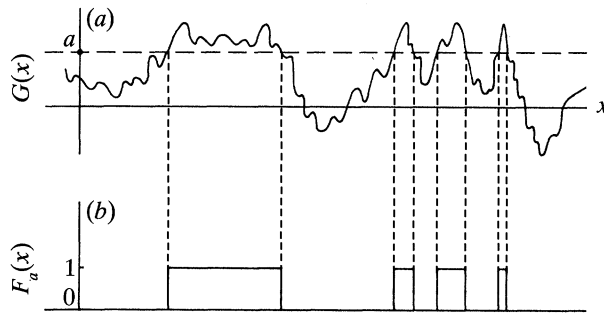


Figure 1. (a) Graph of a continuous non-differentiable random function $G(x)$ for which Orey's formula (3.39) applies (when $G(x)$ follows gaussian statistics at each point x , in which case the graph is H-fractal). This is the particular case $d = 1$; there is only one variable x . (b) If one takes a cut $y = a$ through the previous graph one obtains a square-wave $F_a(x)$. This is also a figure of the on-off function $F(x)$ defined by taking a cut through an interface.

particular non-integer number caused much interest because it was thought that 2.35 might be a fundamental constant of turbulence! (In fact the motions near the edges of clouds are often not characteristic of fully developed turbulence, so it would not be expected that D is a general constant.) This point was perhaps not known to Hentschel & Procaccia who attempted to deduce D from the theory of turbulent diffusion (Hentschel & Procaccia 1984). Unfortunately their work is full of arbitrary premises, one of which appears to be wrong, from the study we describe in this paper. They nevertheless obtained the observed number 2.33. Kingdon (1987) repeated these calculations by changing two of Hentschel & Procaccia's premises and came to the same result.

Lovejoy's work also triggered a further series of experimental measurements of the fractal dimension of various interfaces in turbulent flows, the most well known and complete being those of Sreenivasan and his collaborators (see, for example, Sreenivasan & Meneveau 1986; Sreenivasan *et al.* 1989; Prasad & Sreenivasan 1989). The 'magic' number 2.35 seemed to appear over and over again for different kinds of interfaces embedded in turbulent flows (turbulent jets and wakes, iso-velocity or iso-concentration surfaces, mixing layers, turbulent/non-turbulent interfaces, etc.) an exception being the fractal dimension of turbulent flames (Gouldin 1987; Peters 1988; Chaté 1987; Franke & Peters 1985; Mantzaras *et al.* 1989) which is often smaller than 2.35.

It is interesting that the fractal dimension was either measured or 'deduced' (from the theory of turbulent diffusion) but never explained. As we shall see in the next section, often the dimension that is measured is not the same as the dimension that is thought to be measured. In fact the meaning of D remains largely unclear; especially its connection to the properties of self-similarity and scale-invariance. It so happens that the box counting algorithm (Mandelbrot 1982) provides a measure of what is called a Kolmogorov capacity introduced by Kolmogorov (1958), and subsequently shown to be equivalent to other dimensions, for example, to the Bouligand dimension (see Dupain *et al.* 1983). (It is also often referred to in the literature as box-dimension, similarity dimension, Kolmogorov entropy, or ϵ -entropy. All these denominations refer to the same concept and to equivalent definitions. In calling it a Kolmogorov capacity we follow Farmer *et al.* (1983) and Ruelle (1989). It should not be mistaken for Frostman's capacity (see Falconer 1985).) The Kolmogorov capacity is a number that can be fractional for signals that

have accumulation points without being fractal (i.e. their Hausdorff dimension is equal to their topological dimension). There are examples of spirals that have a Hausdorff dimension of 1 and a Kolmogorov capacity strictly larger than 1.

That Kolmogorov capacity is a convenient measure or identifier of the accumulation patterns discussed by Moffatt (1984). The main aim of this paper will be to take Moffatt's observation described earlier one step further and find the exact relation between the spectrum of a signal that looks like in figure 1*b*, and the character of its accumulation as measured by the Kolmogorov capacity.

(a) *Hausdorff dimensions and Kolmogorov capacities*

It is important to include here a review of how 'fractal' dimensions are defined and measured. A common definition of the 'fractal' dimension of a given geometrical object (e.g. a set of points, a line or a surface) is the following: suppose the object is embedded in a euclidean space of euclidean dimension d (a circle is embedded in a plane of $d = 2$ and a sphere in a space of $d = 3$). Choose a length scale ϵ and cover that object with boxes of size ϵ and 'volume' ϵ^d . $N(\epsilon)$ is the minimum number of such boxes required to cover the object completely. If

$$N(\epsilon) \sim \epsilon^{-D_K} \quad (2.1)$$

for $\epsilon \rightarrow 0$, then the object is often said to be fractal if D_K is a fraction, and D_K is called its fractal dimension. As we shall see these can be misleading statements if by 'fractal' is meant an object with a fractional Hausdorff dimension. The procedure just described is the box counting algorithm (see figure 2).

As for real or numerical experiments the limit $\epsilon \rightarrow 0$ becomes impractical and even illusory (in the real world nothing is 'fractal' down to vanishing length scales), one looks for a range of length scales ϵ between some ϵ_{\max} and ϵ_{\min} where a relation of the type of (2.1) is valid (see figure 3).

The dimension D_K as defined by (2.1) is really called a capacity and was first defined by Kolmogorov in 1958. It is in general not equal to the Hausdorff dimension D_H which is defined as follows: consider a covering of the geometrical object in question with d -dimensional boxes of variable sizes ϵ_i . Define the quantity $H_D(\epsilon)$ by

$$H_D(\epsilon) = \inf \sum_i \epsilon_i^D, \quad (2.2)$$

where the infimum extends to all possible countable coverings subject to the constraint $\epsilon_i \leq \epsilon$. What Hausdorff proved (Hausdorff 1919; see also Falconer 1985) is that as $\epsilon \rightarrow 0$, $H_D(\epsilon)$ tends to either 0 or ∞ according to whether D is larger or smaller than a critical value D_H . That critical value is the Hausdorff dimension and Hausdorff showed that it can be a non-integer number.

It is easily shown that $D_K \geq D_H$ (see, for example, Ruelle 1989). A fractal as defined by Mandelbrot is a geometrical object whose Hausdorff dimension is strictly larger than its topological dimension. We will call such an object an H-fractal. An object whose capacity is strictly larger than its topological dimension but its Hausdorff dimension is not, will be called a K-fractal. In fact we define K-fractals such that a broader class of objects may be included in the definition. It is shown in the Appendix that spirals of the kind $r(\phi) = C\phi^{-\alpha}$ (r, ϕ are polar coordinates on the plane, C and α are constants) with an infinite number of turns and $\alpha > 1$, have a capacity $D_K = 1$ but the set of point intersections of the spiral with a straight line crossing through the centre of the spiral has a non-integer capacity $D'_K = 1/(1 + \alpha)$. (See also last paragraph of §2*c*.) Hence, we define a K-fractal to be a non H-fractal

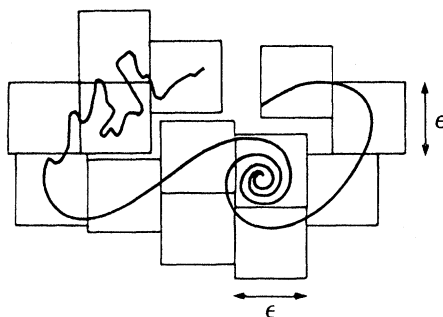


Figure 2. Covering of a line with boxes of size ϵ . That is the first stage of the box counting algorithm.

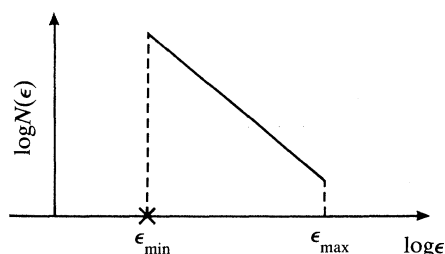


Figure 3. Log-log plot of the minimum number of boxes $N(\epsilon)$ needed to cover the curve in figure 2 against the size ϵ of those boxes. In practice, a power law is only observed in a restricted range of length scales between ϵ_{\min} and ϵ_{\max} .

geometrical object such that there exists a line crossing through it for which the set of point intersections of the object with that line has a Kolmogorov capacity D'_K strictly positive.

It may be that if an object is already known to be H-fractal then $D_K = D_H$. But there is no rigorous and general proof of this. (Falconer (1988) and Bedford & Urbanski (1989) for example, give conditions relating to self-affinity under which they can prove it.) Otherwise, apart from Mandelbrot's statement (Mandelbrot 1982), there is some numerical evidence that the capacity and the Hausdorff dimension of chaotic attractors are equal (Farmer *et al.* 1983). If an object is not yet known to be H-fractal, then (2.1) is by no means a test that can tell us if it is! (Most experimentalists are agnostic about this. Essentially they are concerned with K-fractal processes (see Sreenivasan & Meneveau 1986; Prasad & Sreenivasan 1989; Redondo & Linden 1988; Franke & Peters 1985) and that is not a complete enumeration.) It would be necessary to measure the Hausdorff dimension of that object (or signal) and test whether it is larger than its topological dimension.

The Hausdorff dimension is a direct measure of the 'raggedness' or lack of smoothness of, say, a surface embedded in a three-dimensional euclidean space. If the surface is 'smooth', in the sense that one can define a tangent plane on nearly every point of that surface ('on nearly every point' means 'except on a subset of points of zero area'), then its Hausdorff dimension is equal to its topological dimension, i.e. $D_H = 2$. If not, then $D_H > 2$. When $D_H = 3$, the surface is said to be space-filling because it is so irregular that it fills a three-dimensional region of the three-dimensional euclidean space. D_H cannot be larger than d (in the case of a surface $d = 3$) (see, for example, Ruelle 1989).

The capacity is not a direct measure of the raggedness of a geometrical object. A spiral defined by $r(\phi) = C\phi^{-\alpha}$ for example, has a Hausdorff dimension equal to its topological dimension ($D_{\text{H}} = 1$), but the capacity may be greater than the topological dimension (see the Appendix; D_{K} increases as α decreases). D_{K} is clearly a measure of how quickly the spiral converges onto its centre. If that convergence is slow, α is small and D_{K} is close to 2. If that convergence is fast, α is large and D_{K} is close to 1 (see figure 7).

Note that as $\alpha \rightarrow 0$ and $D_{\text{K}} \rightarrow 2$, the spiral becomes more and more ‘space-filling’ in a sense that is not at all the same as when we say that an H-fractal line of topological dimension 1 and Hausdorff dimension 2 is space-filling. Nevertheless $D_{\text{K}} = 2$ still corresponds to some kind of space-fillingness which, to our knowledge, has not previously been differentiated from the different kind of space-filling property of an H-fractal line for which $D_{\text{H}} = 2$. At the end of this section we note that for K-fractals $D_{\text{K}} \leq d$, which is similar to $D_{\text{H}} \leq d$ for H-fractals. One could formally define K-fractal space-fillingness as being the situation where $D_{\text{K}} = d$, as one can indeed define H-fractal space-fillingness to be equivalent to $D_{\text{H}} = d$. We will now try to give an intuitive understanding of that difference.

The capacity seems to be a good measure of the convergence pattern near an accumulation point or any number of separated accumulation points. In the case of a spiral the accumulation point is obviously its centre, and there is a one to one correspondence between α and D_{K} . That accumulation point is the only ingredient needed for a capacity to be larger than 1.

One accumulation point (or even a finite number of them) is not enough for the Hausdorff dimension to grow larger than the topological dimension. If one looks at an example of an H-fractal set, the triadic Cantor set (see figure 4), one realizes that it has an infinite number of accumulation points in a finite region of the straight line. There are, as it were, accumulations of accumulation points in the neighbourhood of any point of the Cantor set. That is an extremely singular behaviour, which may contain all the information needed to determine the Hausdorff dimension. That accumulation pattern will also be characterized by a value of the capacity strictly larger than the topological dimension of the set, which for the Cantor set is 0 (and it may well be that in such a case the capacity is able to grasp all the fractal aspect of the set and be equal to D_{H} , as is indeed assumed without discussion by various authors (see, for example, Mandelbrot 1982; Voss 1988)).

The space-filling property of a K-fractal line means that as $D_{\text{K}} \rightarrow 2$ the line would tend to fill the space locally, i.e. near an accumulation point or a number of separated accumulation points. On the other hand the space-filling property of an H-fractal line implies that as $D_{\text{H}} \rightarrow 2$ the line become space-filling over a finite continuous region of space. We should also stress the fact that for the Hausdorff dimension to jump above the topological dimension an accumulation of accumulation points is needed, whereas one or a finite number of accumulation points is enough for the capacity to do so. The reason why one finds accumulations of accumulation points in the neighbourhood of every point of an H-fractal, is that it is self-similar everywhere. A K-fractal is self-similar only locally. (Note, as we shall see later, that both kinds of self-similarity produce a power law spectrum: hence, there will be a need in future research for wavelet transforms (see, for example, Grossman & Morlet 1984) to focus on regions where a process is locally self-similar.)

Another way of noting the difference between an H-fractal and a K-fractal for an interface, is that an H-fractal can only be produced by displacements defined by a



Figure 4. The construction of the triadic Cantor set. The initiator is the unit interval $[0, 1]$. The generator removes the open middle third. The figure shows the construction of the five first generations. $D_H = 0.6309$.

large number N_H of parameters (or Fourier components) where $N_H \gg 1$, whereas a K-fractal can be produced by displacements defined by one single number (e.g. the α parameter we defined for spirals). (In fluid mechanics a line placed across a vortex becomes K-fractal; but an H-fractal could only be produced by many eddies at different scales. This is why K-fractals are found in low Reynolds number or transitional flows (Franke & Peters 1985; North & Santavicca 1991). On the other hand there is no conclusive evidence yet that the ‘fractals’ observed at high Reynolds number flows are in fact H-fractals.)

(b) *The volume of H-fractals*

If an object is H-fractal (so its Hausdorff dimension D_H is strictly larger than its topological dimension $E = d - 1$), and if one chooses all ϵ_i in (2.2) to be equal to ϵ (assuming that for H-fractal objects this does not affect the value of $H_D(\epsilon)$ for small enough ϵ , but it can be easily seen to do for K-fractals like a spiral), then one gets

$$H_E(\epsilon) = \inf \sum_i \epsilon^E = N(\epsilon) \epsilon^E \sim \epsilon^{-D'_K}, \tag{2.3}$$

assuming that for H-fractals $D_H = D_K$ and $D'_H = D'_K$, and using the relation $D_H = D'_H + E$ (see Falconer 1985).

$H_E(\epsilon)$ is the ‘ E -volume’ of the E -dimensional H-fractal object measured with resolution ϵ (if $E = 1$, the object is a H-fractal line, and $H_1(\epsilon)$ is its length). We know that it should diverge to infinity as $\epsilon \rightarrow 0$ because $E < D_H$. Equation (2.3) gives the rate of this divergence, and is the original definition of a H-fractal (Mandelbrot 1967).

It is crucial, for an experimental test of H-fractal properties based on (2.3), to measure $H_E(\epsilon)$ according to (2.2) and not by setting all $\epsilon_i = \epsilon$, in which case the test would become simply equivalent to the box counting technique. This point appears to have been neglected in some experimental studies of fractals in turbulence (see, for example, Mantzaras *et al.* 1989; North & Santavicca 1991), and makes an experimental identification of H-fractals based on (2.3) particularly difficult.

Note that (2.3) is not generally valid for K-fractals; for instance, the spirals studied in the Appendix are of finite length when $\alpha > 1$ (see (A 20*b*)) but $D'_K = 1/(1 + \alpha) \neq 0$. For H-fractals $H_E(\epsilon)$ always tends to infinity when $\epsilon \rightarrow 0$!

(A rigorous proof of $D_H = D_K$ if the object is H-fractal, would run along the same lines leading to (2.3), but for a general D instead of E , in order to obtain $H_D(\epsilon) \sim \epsilon^{D-D_K}$ and conclude that $D_K = D_H$ because the threshold value of D for which the limit of $H_D(\epsilon)$ as $\epsilon \rightarrow 0$ jumps from 0 to ∞ , has to be D_H . The delicate point will be to show that by setting all $\epsilon_i = \epsilon$, one does not upset the value of $H_D(\epsilon)$ too much for small enough ϵ . If one neglects that last point one can still say that $H_D(\epsilon) \leq \text{const.} \cdot \epsilon^{D-D_K}$, and deduce rigorously the inequality $D_H \leq D_K$.)

(c) *A new interpretation of the capacity D'_K of a set of points on a straight line*

One can give an alternative definition of the capacity D'_K of a set of points on a straight line, that will prove particularly useful in the next section. Define $n(l)$ to be the probability density for a compact segment of length l to contain no point of the set. If that whole set is contained in a compact segment of length no smaller than L , then, because $N(\epsilon)$ is the minimum number of segments of size ϵ covering the set of points, one can write the following:

$$N(\epsilon)\epsilon + L \int_{\epsilon}^{+\infty} n(l) dl \approx L. \quad (2.4)$$

Differentiating with respect to ϵ and using (2.1) in the form $N(\epsilon) \sim \epsilon^{-D'_K}$, one then comes to the conclusion that, as $\epsilon \rightarrow 0$,

$$n(\epsilon) \sim \epsilon^{-D'_K}. \quad (2.5)$$

The above two relations can be used to show that the capacity D'_K of a set of points has to be smaller than 1 (which also proves that $D'_H < 1$ because $D'_H \leq D'_K$). That is easily done by setting $\epsilon = 0$ in (2.4) and noting, using (2.5), that the integral $\int_0^{+\infty} n(l) dl$ cannot be finite unless $D'_K < 1$.

That result can be generalized to H-fractals of topological dimension E . It is indeed known (see Falconer 1985) that the Hausdorff dimension D'_H of the set of point intersections on a one-dimensional cut through an H-fractal set of Hausdorff dimension D_H and topological dimension E is nearly always $D'_H = D_H - E$. It then follows that

$$D_H < E + 1 = d. \quad (2.6)$$

K-fractals have a similar property, $D_K < E + 1 = d$, which is evident because it is impossible to cover an object in a d -dimensional euclidean space with more than a minimum number $N(\epsilon) \sim \epsilon^{-d}$ of boxes of volume ϵ^d . But no similar theorem is known about one-dimensional cuts through K-fractals. In general, the capacity D'_K of the set of point intersections on a cut through a K-fractal set of topological dimension E and capacity D_K is not equal to $D_K - E$ (see the Appendix, and the example of cuts through K-fractal spirals).

3. The small scale spectrum of K-fractal and H-fractal interfaces

(a) *New result for the spectrum $\Gamma(k)$ in terms of D_K and D_H*

One of the main applications of fractals has been the analysis of interfaces between fluid with different properties, e.g. vorticity, concentration, temperature, reactants, or occurrence of a series of chemical reactions (as in combustion, in which case the interface is a flame, one side of which is burnt and the other unburnt). These can be defined without loss of generality by the boundary between regions where a scalar $F(\mathbf{x})$ is equal to 0 and regions where $F(\mathbf{x}) = 1$. That scalar can only be 0 or 1 everywhere in a d -dimensional space.

The question we will examine in this section is how the capacity D_K or the Hausdorff dimension D_H of that interface relates to the spectrum $\Gamma(k)$ of the scalar function F .

The following analysis starts from two basic assumptions. The first one is that the interface is K-fractal. It does not need to be H-fractal; but the analysis is still valid

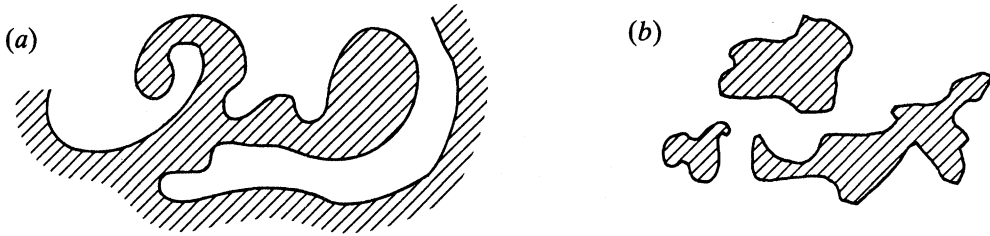


Figure 5. (a) The interface between the shaded and non-shaded regions is connected.
 (b) The interface between the shaded and non-shaded regions is disconnected.

in case it is, provided one trusts the conjecture that for H-fractals $D_K = D_H$. Furthermore, our analysis will be valid for both connected and disconnected interfaces (see figure 5).

The second assumption is that F is statistically homogeneous and isotropic over the scales of interest. That is indeed the case if we assume the turbulence advecting F to be statistically homogeneous and isotropic and the initial profile of F to be also chosen from an homogeneous and isotropic distribution of initial realizations, or to be distributed over space in an isotropic and homogeneous way. We will deal with small-scale averages over space, or over various realizations of the interface that have different orientations and lie in different regions of space (or both). The statistical homogeneity and isotropy of F means that all these realizations have the same weight.

The spectrum $\Gamma(k)$ of F is defined in a series of steps: one first defines the autocorrelation function $c(\mathbf{r})$ of F by

$$c(\mathbf{r}) = \overline{F(\mathbf{x})F(\mathbf{x}+\mathbf{r})}, \quad (3.1)$$

which is actually a function of the modulus $r = |\mathbf{r}|$ only, as F is statistically homogeneous and isotropic. The overbar in (3.1) denotes an average over a large number of realizations, or an average over space \mathbf{x} (or both).

The Fourier transform of $c(\mathbf{r})$, or spectrum function, is

$$S(\mathbf{k}) = \frac{1}{(2\pi)^d} \int c(\mathbf{r}) e^{-i\mathbf{k}\cdot\mathbf{r}} d\mathbf{r}. \quad (3.2)$$

From the inverse transform:

$$c(\mathbf{0}) = \int S(\mathbf{k}) d\mathbf{k}. \quad (3.3)$$

Since $c(\mathbf{r}) = c(r)$, it follows from (3.2) that $S(\mathbf{k})$ is only a function of $k = |\mathbf{k}|$, so one can rewrite (3.3) in the following way:

$$c(\mathbf{0}) = \Omega_d \int_0^{+\infty} k^{d-1} S(k) dk, \quad (3.4)$$

where Ω_d is the d -dimensional solid angle integrated over all directions. It is usual in turbulence to define a power spectrum $\Gamma(k)$ such that

$$c(\mathbf{0}) = \int_0^{+\infty} \Gamma(k) dk. \quad (3.5)$$

Therefore, from (3.4)

$$\Gamma(k) = \Omega_d k^{d-1} S(k). \quad (3.6)$$

The main result of this section will be the following: provided the interface is K -fractal and $c(\mathbf{r}) = c(r)$, then the autocorrelation function of F behaves like a power law over short distances,

$$c(r) - c(0) \sim r^\beta \quad \text{as } r \rightarrow 0, \quad (3.7)$$

where

$$\beta = 1 - D'_K \quad (3.7a)$$

and D'_K is the capacity of the set of point intersections on an arbitrary line cutting through the K -fractal interface that separates regions with different values of F .

The cut can indeed be arbitrary without affecting the value of D'_K because of the homogeneity and the isotropy of the statistics of F . Also because of this isotropy, one can write

$$c(r) = \overline{F(\mathbf{x})F(\mathbf{x} + r\mathbf{e})} \quad (3.8)$$

for any arbitrary vector \mathbf{e} , which means that because of the assumption of homogeneity, one can compute $c(r)$ by only considering the statistics of F on pairs of points on an arbitrary line.

We use the definition (2.5) of D'_K ; we assume that the form of the interface is such that for $\eta < l < L$ some D'_K can be defined on a line. In other words the local accumulation regions extend from some $l = \eta$ to some $l = L$. (η is a function of both the smallest length scale within which sharp gradients of F can be found, and the smallest distance from the convergence point to the line on which D'_K is defined. In the Appendix we show that the set of point intersections of a spiral with a line that does not cross the centre of the spiral has the same D'_K as when the line does cross the centre, but within a slightly smaller range.) The exact decaying behaviour of $n(l)$ for $l > L$ is unimportant because we are interested in results valid for asymptotically small lengths, and $n(l)$, by definition (see §2c), has to be vanishingly small for large l . So, for $l > L$ we set $n(l) = 0$. Normalizing $\int_0^{+\infty} \eta(l) dl$ to 1 (letting $\eta \rightarrow 0$ has no effect on the present analysis and results), leads to:

$$n(l) = ((1 - D'_K)/L) (l/L)^{-D'_K} \theta(L - l), \quad (3.9)$$

where θ is the Heaviside function.

The fact that $F(x)$ is a step function taking either the value 0 or 1 means that $c(r)$ is the probability that both $F(x)$ and $F(x+r)$ are equal to 1. Set $\Pi(r)$ to be the probability that $F(x)$ is equal to $F(x+r)$. Then

$$c(r) = \Pi(r) c(0), \quad (3.10)$$

where $c(0)$ is $\overline{F^2(x)}$, and is also the probability for $F(x)$ to be equal to 1.

$F(x) = F(x+r)$ can occur in a variety of ways which we can describe graphically in figure 6.

Figure 6a is the case for which there is no point element of the interface between x and $x+r$. In figure 6b there are only two points between x and $x+r$ that belong to the interface, and in figure 6c there are four.

An infinite enumeration of all possible ways in which $F(x)$ can be equal to $F(x+r)$ could be constructed. The probabilities attached to each of these possibilities sum up to give an infinite series equal to $\Pi(r)$.

The probability of a graph like figure 6a can be easily calculated if one knows $n(l)$. That probability is

$$\int_r^{+\infty} n(l) dl = \theta(L - r) [1 - (r/L)^{1 - D'_K}]. \quad (3.11)$$

Unfortunately, the exact probabilities to be assigned to all the remaining graphs

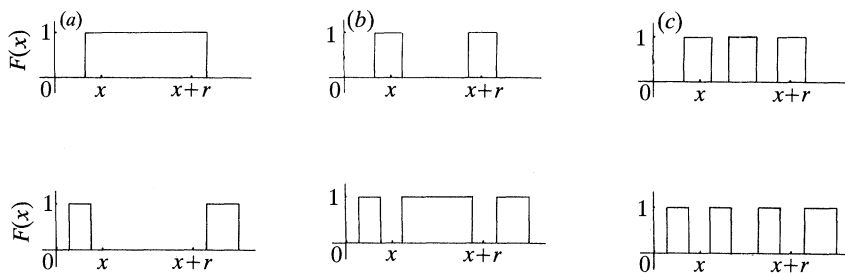


Figure 6.

cannot be determined from $n(l)$ alone. However, as we will now show, the leading contribution to $\Pi(r)$ in terms of powers of (r/L) must come from figure 6a, b. Intuitively this makes sense, because the autocorrelation function is an indication of the ‘persistence’ of the signal F over a certain range of r .

Examine the case of figure 6b: the probability of finding two and only two points of the interface at a distance $l_1 < r$ apart is equal to the probability of finding three convex segments of lengths $l_1 < r, l_2, l_3$ directly bordering each other for any l_2, l_3 such that $l_1 + l_2 + l_3 \geq r$, and with no points of the interface in them except at their two adjoining points. That probability is in turn smaller or equal to the probability of finding three such segments that are not necessarily adjacent, and which can be computed in terms of $n(l)$ in the following way:

$$\int_0^r n(l_1) dl_1 \iint_{r-l_1 \leq l_2+l_3} n(l_2) n(l_3) dl_2 dl_3. \tag{3.12}$$

Carrying out the integration in (3.12) for the case $r \leq L$, leads to:

$$(r/L)^{1-D'_K} - \frac{\Gamma^3(2-D'_K)}{\Gamma(4-3D'_K)} (r/L)^{3-3D'_K}, \tag{3.13}$$

where Γ is Euler’s ‘gamma’ function. The probability of figure 6b being less or equal to (3.13), one concludes therefore that the contribution of that graph to the value of $\Pi(r)$ is at most of the order of $(r/L)^{1-D'_K}$.

Similarly the contribution of a graph like figure 6c will be found to be smaller or equal to

$$\begin{aligned} \int_0^r n(l_1) dl_1 \int_0^{r-l_1} n(l_2) dl_2 \int_0^{r-l_1-l_2} n(l_3) dl_3 \iint_{l_4+l_5 \leq r-l_1-l_2-l_3} n(l_4) n(l_5) dl_4 dl_5 \\ = \frac{\Gamma^3(2-D'_K)}{\Gamma(4-3D'_K)} (r/L)^{3-3D'_K} - \frac{\Gamma^5(2-D'_K)}{\Gamma(6-5D'_K)} (r/L)^{5-5D'_K}. \end{aligned} \tag{3.14}$$

The next graph after figure 6c, which we have not drawn and which involves seven integrations will not contribute more than

$$\frac{\Gamma^5(2-D'_K)}{\Gamma(6-5D'_K)} (r/L)^{5-5D'_K} - \frac{\Gamma^7(2-D'_K)}{\Gamma(8-7D'_K)} (r/L)^{7-7D'_K} \tag{3.15}$$

((3.14) and (3.15) are only valid for $r \leq L$).

Notice that if one adds up (3.11), (3.13), (3.14), (3.15) and all the remaining upper bounds of higher contributions to $\Pi(r)$, one gets

$$\Pi(r) \leq 1 \tag{3.16}$$

as expected.

It is now clear that the largest contribution to $\Pi(r)$ comes from figure 6*a, b*, and is of order $(r/L)^{1-D'_K}$. In fact, for $r \ll L$,

$$\Pi(r) \approx 1 - A(r/L)^{1-D'_K} \tag{3.17}$$

and $A < 1$.

Likewise, for $r \ll L$,

$$c(r) \approx c(0) [1 - A(r/L)^{1-D'_K}] \tag{3.18}$$

(note that this method does not allow us to determine the value of A , except that it is smaller than 1).

Taking the Fourier transform (3.2) of (3.18) with a suitable change of variables ($r' = kr$) and using (3.6), we obtain the basic result of this section:

$$\Gamma(k) \sim k^{-2+D'_K}. \tag{3.19a}$$

It is valid for large enough wavenumbers (i.e. $k \gg 2\pi/L$) under the assumption that F is statistically homogeneous and isotropic, and that the surface of discontinuity of F is either K-fractal or H-fractal. Indeed, if it is H-fractal, then the previous analysis can be identically reproduced with $D'_K = D'_H$, which is the Hausdorff dimension of the set of point intersections of the interface with an arbitrary cut. In this case one can also rewrite (3.19*a*) in terms of the Hausdorff dimension D_H of the entire interface ($D_H > E$) because $D_H = D'_H + E$ for nearly all cuts through the interface (see Falconer 1985):

$$\Gamma(k) \sim k^{-2-E+D_H}. \tag{3.19b}$$

When the interface is K-fractal, (3.19*a*) cannot in general be trivially reformulated in terms of the Kolmogorov capacity D_K of the entire interface ($D_K \geq E$). In fact, in general, $D_K \neq D'_K + E$. But as we show in the Appendix, for K-fractal spirals $D_K = D'_K + E$ in a limited range of resolutions ϵ where no more than approximately five to six turns of the spiral can be resolved. At much finer resolutions the calculated (or computed) value of D_K is not equal to $D'_K + E$. If we assume an homogeneous and isotropic distribution of spirals of not more than a few (*ca.* 5) turns on the interface (the statistics of F are assumed to be homogeneous and isotropic), then computations and analysis indicate that there is a range of resolutions ϵ where $D_K = D'_K + E$. In that case, it follows that

$$\Gamma(k) \sim k^{-2-E+D_K}. \tag{3.19c}$$

The distribution of spirals may be such that there exists a cascade of smaller spirals upon larger spirals; that cascade may be H-fractal, in which case (3.19*c*) is the same as (3.19*b*), because then $D_H = D_K$. The distribution of spirals need not be of this type though; it can simply be an homogeneous and isotropic distribution of well separated spirals of variable sizes (do not confound the size of the spiral and its number of turns), and therefore be K-fractal, in which case (3.19*c*) applies but not (3.19*b*) because $D_H = E$.

The analysis leading to (3.19) can be generalized for the n th derivative of F , if it is the n th derivative of F that has the profile of a step function and all lower derivatives are continuous. In that case F is a piecewise C^∞ polynomial of the n th order, and its spectrum $\Gamma_n(k)$ can be shown to be of the form (3.19) where the power $(-2 + D'_K)$ will have to be replaced by $(-2 - 2n + D'_K)$, i.e.

$$\Gamma_n(k) \sim k^{-2-2n+D'_K}. \tag{3.20}$$

The implication of (3.19*a*) and (3.19*b*) is that a unique value of D'_K or of D_H can be deduced from the power spectrum of the function F , assumed to be discontinuous

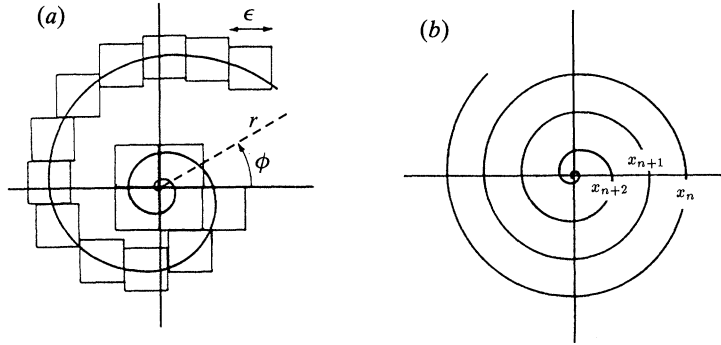


Figure 7. (a) A spiral with the x axis cutting through it. (r, ϕ) are polar coordinates. Here, D_K is close to 1 and α is large. (b) A spiral with D_K close to 2 and α close to 0. x_n is the series of points obtained by cutting through the spiral.

through either a H-fractal interface or a K-fractal interface that is homogeneous and isotropic. In particular if $\Gamma(k) \sim k^{-p}$ and $p < 2$, then $D'_K > 0$, and accumulation points exist, which may or may not be associated with spiral geometry. If the interface is made of an homogeneous and isotropic distribution of spirals of not more than five turns then a unique value of D_K can be deduced from (3.19c).

Moffatt's specific spiral example (Moffatt 1984) is a special case of (3.19a). His method shows that the spectrum of a one-dimensional on-off function obtained by taking a cut through the centre of a spiral of type $r(\phi) \sim \phi^{-\alpha}$ (polar coordinates, see the Appendix) is given by

$$\Gamma(k) \sim k^{-2+1/(1+\alpha)}$$

which is consistent with (3.19a) because (see the Appendix) the Kolmogorov capacity of the point intersections on that cut is given by $D'_K = 1/(1+\alpha)$.

(b) *An accurate measure of self-similarity*

We have shown (3.18) to be valid for $r \ll L$. In reality though, the interface is K-fractal or H-fractal in a range of scales between some ϵ_{\min} and L . One expects, therefore, the range of scales in which $c(r)$ has a power law dependence on r to be also bounded from below, but it is unclear whether this lower bound is the same as ϵ_{\min} or if it is smaller or larger. Here we focus on interfaces at an accumulation point which have the geometrical form $x_n \sim n^{-\alpha}$ ($\alpha > 0$) (see figure 7), to analyse how these two ranges of length scales compare.

Figure 8a shows the accumulation pattern of the intersections $(x_n, 0)$ of a spiral with the x axis taken to cut through the centre of that spiral. If the spiral is of the kind discussed in the Appendix, then

$$x_n \sim n^{-\alpha}, \quad (3.21)$$

where α is some positive real number. Spiral singularities are therefore an example of the type of singularities we are analysing.

The on-off function $F(x)$ corresponding to the series x_n is defined by:

$$F(x) = \sum_{p=1}^{+\infty} h_p(x) \quad (3.22a)$$

and h_p is a product of two Heaviside functions (see figure 8);

$$h_p(x) = H(x - x_{2p})H(x_{2p-1} - x). \quad (3.22b)$$

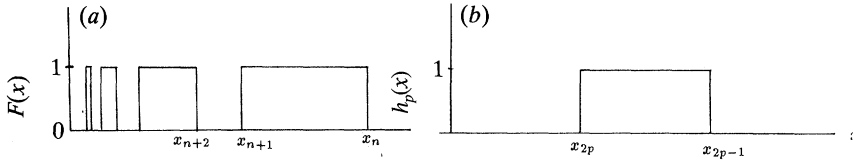


Figure 8. (a) The on-off function $F(x)$ corresponding to the series x_n drawn in figure 7. (b) The function $h_p(x)$ defined in (3.22b).

We take the autocorrelation function $c(r)$ to be

$$c(r) \propto \int F(x) F(x+r) dx \tag{3.23}$$

in accordance with (3.1), provided we choose to give the meaning of a space average to the overbar involved in (3.1).

From (3.23) and (3.22a) we get:

$$c(r) \propto \sum_{p=1}^{+\infty} \sum_{q=1}^{+\infty} \int h_p(x) h_q(x+r) dx. \tag{3.24}$$

The product $h_p(x) h_q(x+r)$ vanishes unless the following inequalities hold:

$$x_{2p} \leq x \leq x_{2p-1} \quad \text{and} \quad x_{2q} \leq x+r \leq x_{2q-1}. \tag{3.25}$$

For that to be at all possible when x_n is a decreasing function of n (which is indeed the case here), and if we assume $r \geq 0$ (which is not restrictive), we must have $q \leq p$. If $q < p$, it is also necessary that

$$x_{2q} - x_{2p-1} \leq r \leq x_{2q-1} - x_{2p} \tag{3.26a}$$

and if $q = p$, the necessary condition for inequalities (3.25) to hold is

$$x_{2p-1} - x_{2p} \geq r. \tag{3.26b}$$

We can now be a little more precise on the range over which the summation in (3.24) is effectively carried out without adding vanishing terms; the summation over p can be restricted to values higher than q , i.e.

$$c(r) \propto \sum_{q=1}^{+\infty} \sum_{p \geq q}^{+\infty} \int h_p(x) h_q(x+r) dx. \tag{3.27}$$

Furthermore, a particular consequence of inequalities (3.26) is that the above summation over q need not be carried to infinity. The highest value of q for which $h_p(x) h_q(x+r)$ can be non-zero is given by $x_{2q} \sim r$, and is therefore approximately equal to $\frac{1}{2}r^{-1/\alpha}$. So (3.27) becomes,

$$c(r) \propto \sum_{q=1}^{\frac{1}{2}r^{-1/\alpha} + \infty} \sum_{p \geq q}^{+\infty} \int h_p(x) h_q(x+r) dx. \tag{3.28}$$

In practice the series x_n is not infinite. The series has only a number N of elements corresponding, for example, to a spiral with only N turns, and x_N is the element of the series observed to be the closest to 0. When that is the case, the only values of r for which $c(r)$ can be calculated with good accuracy are, according to (3.28),

$$\frac{1}{2}r^{-1/\alpha} < N, \tag{3.29}$$

i.e.
$$r > (2N)^{-\alpha}. \tag{3.30}$$

In the limit $N \gg \frac{1}{2}r^{-1/\alpha}$, the error $\delta c(r)$ on $c(r)$ is then given by

$$\delta c(r) \propto \sum_{p>N}^{+\infty} \int h_p(x) dx, \tag{3.31}$$

where the sum $\sum_{q=1}^{\frac{1}{2}r^{-1/\alpha}} h_q(x+r)$ has been omitted because it is equal to 1. N is indeed large enough for the function $h_q(x+r)$ corresponding to $q = \frac{1}{2}r^{-1/\alpha}$ to be equal to 1 for those values of x for which one of the functions $h_p(x)$ ($p > N$) does not vanish. Equation (3.31) is then reduced to

$$\delta c(r) \propto \sum_{p>N}^{+\infty} \int_{x_{2p}}^{x_{2^{p-1}}} dx \sim \alpha \sum_{p>N}^{+\infty} \frac{1}{(2p)^{\alpha+1}}, \tag{3.32}$$

which is of order $(2N)^{-\alpha}$. Thus we obtain

$$\delta c(r) = O(1/(2N)^\alpha) \tag{3.33}$$

and it should be emphasized that the error on the correlation function $c(r)$ will be even larger if r is of the order or smaller than $(2N)^{-\alpha}$.

N also determines the smallest resolution ϵ_{\min} down to which the box-counting algorithm can be used for this locally self-similar function. That is

$$\epsilon_{\min} \sim x_{N-1} - x_N, \tag{3.34}$$

which by use of (3.21) for very large values of N ($N \gg 1$) becomes

$$\epsilon_{\min} \sim \alpha/N^{\alpha+1}. \tag{3.35}$$

From (3.30) one can conclude that if the series $x_n \sim n^{-\alpha}$ is resolved down to its N th component (with a resolution ϵ_{\min} given by (3.35)) so as to make it possible to differentiate between x_n and x_{n-1} for all $n \leq N$, then $c(r)$ can only be calculated ‘accurately’ (with an accuracy of $O(\epsilon_{\min}^{\alpha/(\alpha+1)})$) within a range of r that is bounded from below by

$$(\epsilon_{\min})^{\alpha/(\alpha+1)} \leq r. \tag{3.36}$$

By using the fact that $D'_K = 1/(1+\alpha)$ (Appendix), this result shows that the range of r for which the autocorrelation of $c(r)$ has the self-similar power law relation (3.7) differs from the range of r over which D'_K is defined. Also, the error in $c(r)$ associated with this finite range of r can be stated in terms of D'_K .

Condition for calculating D'_K :

$$\epsilon_{\min}/L \sim (x_N/x_0)^{1/(1-D'_K)} \ll 1. \tag{3.37}$$

Condition for $c(r)$ to satisfy (3.7): $x_N < r < x_0 \sim L$, where

$$(\epsilon_{\min}/L)^{1-D'_K} \sim x_N/x_0 \ll 1, \tag{3.38a}$$

with error

$$\delta c(r) = O((\epsilon_{\min}/L)^{1-D'_K}). \tag{3.38b}$$

Thus as the spiral becomes more tightly wound (i.e. α decreases and D'_K increases), the range of r required for $c(r)$ to have the self-similar form (3.7) becomes much greater than the range required for a satisfactory measure of D'_K .

The conclusion is that a measure of (local) self-similarity based on spectra/correlation methods is less reliable than one based on the box-counting algorithm and the measure of the Kolmogorov capacity. From the above argument, the main

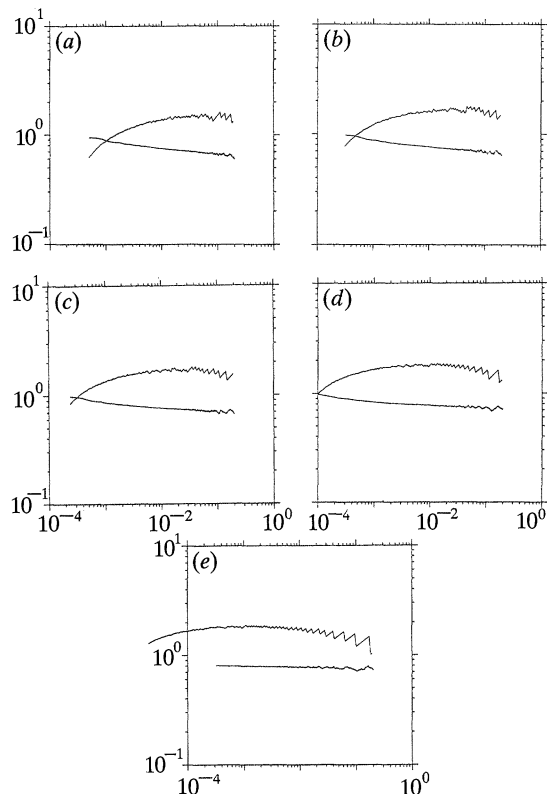


Figure 9. Log-log plots of $(c(0)-c(r))/r^{1-D'_K}$ (lower curve) and $N(\epsilon)\epsilon^{D'_K}$ (upper curve), where $N(\epsilon)$ is given by (2.1) and is the number of boxes needed to cover the point intersections of the spiral with the x axis. (a) $\alpha = 0.5$, $D'_K = 0.66$. (b) $\alpha = 0.66$, $D'_K = 0.60$. (c) $\alpha = 0.75$, $D'_K = 0.57$. (d) $\alpha = 1$, $D'_K = 0.5$. (e) $\alpha = 1.5$, $D'_K = 0.4$. The power law (3.18) is clearly observable in a range of length scales bounded from above by 0.2 and from below by (approximately): (a) 60%, (b) 80%, (c) 86%, (d) 95%, (e) 99% of the total extent 0.2 to ϵ_{\min} in which we resolved the spirals. As predicted by (3.38), that percentage increases as D'_K decreases.

reason for this seems to be that the box counting algorithm is sensitive to the distance between consecutive elements of the series accumulating on 0 (see (3.34)), while the autocorrelation function is primarily sensitive to the distance of each one of these elements to 0 (see (3.30)). The capacity appears therefore to be a natural and direct measure of the self-similarity of the spacings between folds of an interface, whereas $c(r)$ and $\Gamma(k)$ are indirect measures.

Note also that (3.19) enables the form of $\Gamma(k)$ to be estimated in the limit where it has a power law form, because D'_K can be measured accurately in a parameter range where $\Gamma(k)$ does not have an accurate (or a single) power law form.

A numerical computation of the correlation function $c(r)$ and the Kolmogorov capacity D'_K of the set of point intersections of a spiral with the x axis is a good illustration of some of the points in this §3. We examine five cases of a spiral with different convergence patterns; $\alpha = 0.5, 0.66, 0.75, 1.0, 1.5$, according to (A 1). We find the numerically computed values of D'_K to be in good agreement with (A 9), in an intermediate range of length scales between ϵ_{\min} and ϵ_{\max} . We set $\epsilon_{\max} = 0.2$ in all five cases (see figure 9). We resolve 99 turns of the spiral for each case, i.e. we keep (see (A 2)) r_1, r_2, \dots, r_N with $N = 100$. This means that we resolve each of these spirals

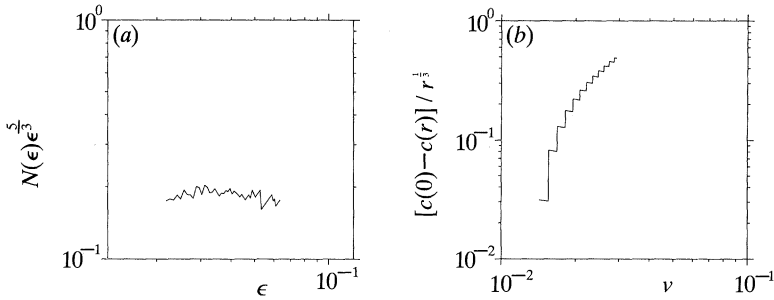


Figure 10. (a) A log-log plot of $N(\epsilon)\epsilon^{D_K}$ against ϵ , for only two turns of a spiral $r(\phi) \sim \phi^{-\frac{1}{2}}$ for which $D_K \approx 1.66$ in the range resolved (see (A 25)). The distance between turns varies between 10^{-1} and roughly 0.510^{-2} . $N(\epsilon) \sim \epsilon^{-1.666}$ in a range between $10^{-1.3}$ and $10^{-1.8}$. (b) A log-log plot of $(c(0) - c(r))/r^{0.333}$ against r for only two turns of the same spiral.

down to a scale ϵ_{\min} that is different for each one of them (see (3.34) and (3.35)); $\epsilon_{\min} \approx 0.5 \times 10^{-3}, 0.3 \times 10^{-3}, 0.24 \times 10^{-3}, 10^{-4}, 0.15 \times 10^{-4}$ as $\alpha = 0.5, 0.66, 0.75, 1.0, 1.5$.

The numerical computation of $c(r)$ based on a resolution $N = 100$, fits the analytical result (3.18) in a range that is, as we expected, progressively smaller for increasing D'_K . The power law (3.18) seems to be numerically measurable in a range of length scales bounded from above by 0.2, and bounded from below by (approximately) 0.08, 0.04, 0.028, 0.01 and 0.0013 for the respective values of $\alpha = 0.5, 0.66, 0.75, 1.0, 1.5$. These values of α correspond to decreasing Kolmogorov capacities $D'_K = 0.66, 0.60, 0.57, 0.5, 0.4$. This increase of the range of experimental 'validity' of (3.18) with decreasing D'_K is in good quantitative agreement with inequality (3.37). This is clear in figure 9, which give us the additional information that a calculation of a correlation function with only finite resolution overestimates the relative magnitude of $c(r)$ at small scales r (smaller than $\epsilon_{\min}^{1-D'_K}$, see (3.37)) in comparison with its magnitude at larger scales.

A more dramatic illustration of (3.37) and of the impossibility of measuring the asymptotic form of the spectrum $\Gamma(k)$ of a spiral interface that has only a few turns is given in figure 10. We measure numerically the capacity D_K of an entire spiral of only two turns and find the correct value of D_K in agreement with (A 25) (figure 10a). But a measure of the correlation function $c(r)$ does not reveal the self-similar form of $c(r)$ (figure 10b). Clearly, from (3.33), the error on $c(r)$ is $O(1)$ in this case. But on the basis of only two turns of the spiral D_K can be measured, and thence using (3.18) (and (A 26)), the asymptotic form of $c(r)$ can be derived indirectly for the situation when the spiral has a large or infinite number of turns.

There is of course an additional well-known problem in the calculation of the spectrum $\Gamma(k)$; that is the Gibbs phenomenon (see Bracewell 1986), which arises from 'fitting' a discontinuous function – here a square wave (see figures 1b, 7a) – to a series of sinus/cosinus functions. That is another source of errors, independent of the previous one and specifically due to the discontinuities in F (but not their accumulation). The shortening of the range where $c(r)$ has a power law dependence on r is the consequence of the self-similar accumulation of these discontinuities. This shortening is gradually more pronounced as the folds of the interface (or the accumulation of the discontinuities of F) become more space filling (i.e. as $D'_K \rightarrow 1$ in (3.37)).

(c) *Review of previous results*

A similar result to (3.19*b*) was derived by Orey (1970). It applies to gaussian random functions $G(\mathbf{x})$ that are quite different from the ones considered here. These functions are continuous in \mathbf{x} and such that the hypersurface $y = G(\mathbf{x})$ defined in the $(d+1)$ -dimensional $(y, x_1, x_2, \dots, x_d)$ -space is H-fractal (see figure 1*a*). Let Δ_{H} be the Hausdorff dimension of the hypersurface; Orey's result for the spectrum of such functions can then be written as

$$\Gamma(k) \sim k^{-3-2d+2\Delta_{\text{H}}}. \quad (3.39)$$

It should be stressed that if the hypersurface $y = G(\mathbf{x})$ is not H-fractal then the spectrum of G is not given by (3.39), even if it has a Kolmogorov capacity that is larger than its topological dimension (which is d). One cannot replace Δ_{H} in (3.39) by a Kolmogorov capacity (unless, of course, that Kolmogorov capacity is equal to Δ_{H}).

Hentschel & Procaccia (1984) applied Orey's formula (3.39) to scalar on-off functions. They considered the intersection in the $(d+1)$ -dimensional $(y, x_1, x_2, \dots, x_d)$ -space of the hypersurface $y = G(\mathbf{x})$ (assumed to be H-fractal, and G assumed to be continuous) with an arbitrary hyperplane $y = a$. This procedure defines the on-off function $F_a(\mathbf{x})$ (see figure 1*b*),

$$F_a(\mathbf{x}) = \theta(F(\mathbf{x}) - a) \quad (3.40)$$

and the previous intersection is the interface separating in d -dimensional \mathbf{x} -space, regions where $F_a = 1$ from regions where $F_a = 0$. Such an intersection is nearly always H-fractal with Hausdorff dimension $D_{\text{H}} = \Delta_{\text{H}} - 1$ (see Falconer 1985). Hentschel & Procaccia used the substitution $\Delta_{\text{H}} = D_{\text{H}} + 1$ in (3.39) so as to obtain

$$\Gamma(k) \sim k^{-3-2E+2D_{\text{H}}},$$

which differs from the correct result for the spectrum of F_a given by (3.19*b*). Their error was in the unjustified application to discontinuous functions of the result (3.39), which is only valid for continuous functions.

Kingdon (1987) was the first to propose the result (3.19*b*). He used an essentially scaling argument that depends crucially on interpreting the average involved in the definition (3.1) of $c(\mathbf{r})$ as a space average. As we saw, that is in fact not necessary. Also, he did not seem to be aware of the difference between D_{K} and D_{H} , and therefore thought that (3.19) was valid only for H-fractals.

Another illustration of the difference between formulas (3.19*b*) and (3.39) comes from a comment on a paper by Mandelbrot (1975), where he discusses the Hausdorff dimension of isosurfaces of continuous gaussian random scalar fields in a three-dimensional space. He states that if the spectrum of the scalar is k^{-2} the Hausdorff dimension is 2.5 (that was first proved by Taylor in 1954), and if the spectrum is $k^{-\frac{5}{3}}$ it is 2.66. Both these results are direct consequences of Orey's formula (3.39), and are valid for continuous signals. But such fractional spectra can also be formed by discontinuities in the signal. In that case Orey's formula cannot be used. If the signal is an on-off function in three-dimensional space (obtained as in (3.40) for example) and if its spectrum is k^{-2} or $k^{-\frac{5}{3}}$, then by application of (3.19*b*) or (3.19*c*), the Hausdorff dimension or the capacity of the surface where the signal is discontinuous (assumed to be respectively either H-fractal or K-fractal with an isotropic and homogeneous distribution of spirals with a few turns) is 2 for the k^{-2} spectrum and 2.33 for the $k^{-\frac{5}{3}}$ spectrum.

Whether interfaces in turbulent flows with $k^{-5/3}$ spectra have a Hausdorff dimension 2.66 or a capacity 2.33 depends on whether turbulent interfaces can be described as isosurfaces of a H-fractal continuous gaussian signal or as H- or K-fractal surfaces of discontinuity of an on-off function. As we shall now see, it is the second case that seems to agree with experiments.

4. Applications in turbulence

Experiments mixing, say, a blob of dye in a turbulent velocity field usually start with the clear cut situation in which all the dye is homogeneously spread in a particular region of space and totally absent in the rest. As explained in the introduction, an on-off function of the kind used to derive (3.19) is the natural choice of function to describe this initial situation, and actually remains so for quite some time until diffusive effects become important. When that happens the sharp discontinuities of the on-off function become smoothed out, and the signal decays, so that fluctuations with a characteristic length scale are lost. The signal has therefore been transformed to a continuous signal. It looks very smooth (everywhere differentiable) when looked at with a resolution smaller than the diffusive length scale, but is still very irregular when looked at with higher resolutions (it may then appear to be nowhere differentiable). It is not clear though whether it is H-fractal or K-fractal (or maybe even neither). Only if the continuous signal is H-fractal and gaussian can the formula (3.39) be applied to it. Over small length scales it is not a good approximation to assume the scalar has a gaussian distribution, and therefore (3.39) cannot be applied.

Also, there is numerical evidence that accumulation patterns of on-off signals in two-dimensional turbulence are K-fractal with spiral structures but not H-fractal (Vassilicos 1989; Jiménez & Martel 1991). It is unlikely that an initial on-off signal with a K-fractal (and non H-fractal) accumulation pattern can eventually become H-fractal through the action of molecular diffusion.

Furthermore, there is no convincing evidence that interfaces in three-dimensional turbulence become H-fractal. As mentioned in the previous section, experimentalists have been measuring the Kolmogorov capacity rather than the Hausdorff dimension, and have never tested (by blowing up their digitized pictures, for example) whether these interfaces are self-similar at local accumulation points only (i.e. K-fractal) or everywhere (i.e. H-fractal).

Power shaped forms of spectra of on-off functions occur in a wide range of situations in turbulent flows. Equation (3.19c) can therefore be applied to them, to find the value of D_K of a given interface that is assumed (or experimentally known) to be K-fractal with an homogeneous and isotropic distribution of spirals of a few turns. (Equivalently, (3.19b) can be used to find the value of D_H of an interface that is assumed or known to be H-fractal.)

Burger's one-dimensional $x-t$ equation for a continuous variable (Saffman 1968) generates one-dimensional 'shocks' or discontinuities and a k^{-2} spectrum. Because finite discontinuities exist, (3.19a) can be used. Its application yields $D_K = E = 0$ which implies that the shocks do not accumulate, i.e. they remain separated. (Note that a k^{-2} spectrum does not necessarily imply shocks.)

In two-dimensional turbulence Kraichnan (1967) and Batchelor (1969) argued that on scales where viscosity is negligible the vorticity spectrum is $\Omega(k) \sim k^{-1}$.

Theoretical suggestions and computer simulations (Kida 1985; Brachet *et al.* 1986) now show that there are distinct thin regions of high gradients of vorticity. Outside these regions, the magnitude of the vorticity does not vary much (viscous stresses are negligible). (In inviscid two-dimensional flows the vorticity on fluid elements is constant and cannot be amplified anywhere.)

Therefore, at small scales, the vorticity spectrum $\Omega(k)$ is approximately identical to the spectrum $\Omega_I(k)$ of interfaces between regions of finite and low vorticity, i.e. $\Omega_I(k) \approx \Omega(k) \sim k^{-1}$. It is appropriate to apply (3.19*a*), and hence one obtains the value of $D'_K = 1$, which implies that in two-dimensional turbulence accumulation points exist within which the vorticity interface is space-filling. Computer simulations certainly show these accumulation regions where the vortex sheets tend to be space-filling (Kida 1985; Brachet *et al.* 1986).

For decaying two-dimensional turbulence Saffman (1971) argues that the vorticity spectrum $\Omega(k)$ will be of the form k^{-2} . Insofar as one can consider advection of vorticity as equivalent to advection of a passive scalar that can only take the values 0 or 1, then (3.19*a*) applies and gives $D'_K = 0$ for the set of discontinuities between high vorticity regions and low vorticity regions. That is indeed the case considered by Saffman, for in his argument he assumes those discontinuities never to accumulate.

Gilbert (1988*a*) has analysed the accumulation of such discontinuities, and has shown that a spiral formed by the passive advection of a weak patch by a strong vortex has a vorticity spectrum of $k^{-\frac{5}{3}}$. That is $D'_K = 0.33$.

Another example of occurrence of power shaped spectra is the three-dimensional turbulent convection of a passive scalar. Batchelor (1959) has shown the spectrum of such a scalar to be $k^{-\frac{5}{3}}$ in the inertial subrange and k^{-1} in the convective-inertial subrange when the ratio Pr of kinematic viscosity ν to diffusivity κ is very much larger than 1.

In the absence of molecular diffusion (infinite Prandtl number Pr and vanishing Batchelor length scale), and subject to the right initial conditions, such a passive scalar can indeed be regarded as a step function F equal to either 0 or 1. That still holds as a good approximation if the molecular diffusivity of the scalar is extremely small, and if one does not resolve length scales of the order of magnitude of the Batchelor length scale. According to (3.19*a*) the interface (assumed to be K -fractal with spiral structures of a few turns) between regions where $F = 1$ and regions where $F = 0$ has a line capacity $D'_K = 1$ in the k^{-1} case, and $D'_K = 0.33$ in the $k^{-\frac{5}{3}}$ case. The capacities D'_K of the intersections of straight lines with interfaces has been measured in a number of different turbulent flows (see Sreenivasan & Meneveau 1986; Sreenivasan *et al.* 1989). They found that in all these flows $D'_K = 0.33$ for the larger length scales and $D'_K = 1.0$ for very small length scales. We note that these authors did not measure the spectrum of F . In fact for the Reynolds number of their experiment the high Reynolds number spectra would not be expected (and neither would high Reynolds and Schmidt number similarity principles apply). However, we have shown by (3.38) that even when the asymptotic high Reynolds form of the spectra is not found, the capacity may still have the asymptotic value.

Experimental measurements of spectra (see, for example, Gibson 1963) of scalars confirmed Batchelor's theoretical model and also photographs of scalars in turbulent flow when $Pr \sim 10^3$ (see, for example, Sreenivasan *et al.* 1989; Dimotakis *et al.* 1981) are consistent with the hypothesis of discontinuous interfaces. Furthermore the photographs do not indicate the kind of global self-similarity measured by a

Hausdorff dimension; rather they are consistent with a local self-similar spiral structure measured by a capacity D_K . A model of this process was investigated by calculating D_K for material lines in a simulated two-dimensional turbulent velocity field (Vassilicos 1989). This showed that D_K is only non-integer near spiral accumulation points, and therefore these points determine the value of D_K for a general line or surface in a turbulent flow. Consequently it is appropriate to compare the calculation of D_K from the spectrum using (3.19c) with the measurement of D_K using the box counting algorithm.

Sreenivasan & Meneveau (1986) have measured the capacities D_K and D'_K of interfaces in turbulent flows and their intersections with straight lines or planes, and found $D'_K = D_K - E$. They interpreted this result by assuming the interfaces to be H-fractal, in which case the Hausdorff dimensions D_H and D'_H are expected to be equal to the respective Kolmogorov capacities (i.e. $D_H = D_K$, $D'_H = D'_K$), and $D'_H = D_H - E$ is indeed valid for nearly all plane or line intersections through a H-fractal (Falconer 1985). But if interfaces in turbulent flows are K-fractal rather than H-fractal, then $D'_K = D_K - E$ is not a trivial property and can be explained by assuming the K-fractal interfaces to be made of K-fractal spirals of a few turns (less than approximately five or six turns, see the Appendix).

Sreenivasan *et al.* (1989) explained their measured values of D_K by constructing a physical model of the diffusive processes over small scales in fully developed turbulence, using scaling arguments appropriate for large values of Reynolds and Schmidt numbers.

Finally, there is an example of a power shaped spectrum for which (3.19) does not apply. That is the convective subrange spectrum $k^{-\frac{17}{3}}$ for a passive scalar in a turbulent medium when the Prandtl number is negligible compared with 1 (Batchelor *et al.* 1959). That spectrum is primarily due to molecular diffusion, hence its very steep fall-off. Any sharp edges are smeared off and one cannot think any longer in terms of step functions.

5. Conclusions

We have made a distinction between two types of self-similarity which is pertinent for problems of interfaces in fluid flows: a local and a global self-similarity.

The first is a property of what we call K-fractals, and the second is a property of H-fractals. K-fractals have a Kolmogorov capacity D'_K of the set of point intersections on at least one linear cut that is strictly larger than 0 and H-fractals have a Hausdorff dimension D_H that is strictly larger than E . The capacities D_K and D'_K can be easily determined from the box-counting algorithm. Furthermore, D_K is a measure of self-similarity that can be applied to H-fractals too; it is believed that for H-fractals, $D_H = D_K$.

The spectrum of the interface (or more accurately, the spectrum of a scalar function that is abruptly discontinuous across the interface) is a more traditional measure of self-similarity. We find a one-to-one relation between the capacity D'_K of the set of point intersections on a linear cut through the interface and the small scale spectrum of the interface that is assumed to become K-fractal through the action of the flow. The flow need not be turbulent for that assumption to hold. K-fractals have not only been observed in turbulent flows, but they can also be generated by simple one-parameter laminar flows, e.g. a single vortex. The study of K-fractals is therefore of much broader relevance than the study of H-fractals. In fact it is not even clear yet whether H-fractals exist in turbulent flows.

Specifically, we show that under some conditions of statistical homogeneity and isotropy, the small-scale spectrum of K-fractal and H-fractal interfaces obeys a power law and we give the relation between that power and, respectively, the Kolmogorov capacity or the Hausdorff dimension of the interface. It is of particular interest that the self-similarity of the interface need not be global for its spectrum to be a power law. A single spiral singularity on the interface is enough.

Conditions for the existence of self-similarity based on spectrum methods are less reliable than when based on the Kolmogorov capacity, because the range of length scales over which a correlation can be accurately calculated is significantly smaller than the range of length scales where the interface is self-similar (and over which the capacity is defined and measured). This shows that the value of D_K can approach closely the asymptotic value for a particular flow structure even when, for the same interface, the spectra do not approximate at all closely their asymptotic form. Consequently the value of D_K may be more sensitive than the traditional power spectra in indicating that some aspects of the structure of the turbulence are close to their asymptotic form for high Reynolds number.

We have used our calculation to interpret and relate the spectra and capacity of a number of flows where power law spectra are found. The theory is confirmed experimentally and also provides a few interpretations of the flow structure in terms of space-fillingness and spiral accumulation points.

We are grateful for very fruitful discussions with A. D. Gilbert, H. K. Moffat, C. Meneveau, K. R. Sreenivasan and U. Frisch. With regard to the Appendix, we acknowledge A. A. Kerstein, M. Borgas, P. Dimotakis and in particular J. Jiménez for bringing (A 22) to our attention. J. Jiménez also impressed on us that $D'_K = D_K - E$ is not generally true. M. Mendes France has been very helpful in clarifying these issues. We have also benefited from T. Bedford's comments on §2. This work has been financially supported by an E.C. contract no. ST2J-0029-1-F.

Appendix. The Kolmogorov capacity of spirals

The aim of this Appendix is to calculate the Kolmogorov capacity D_K of a spiral defined by

$$r(\phi) = C\phi^{-\alpha}, \quad (\text{A } 1)$$

where (r, ϕ) are polar coordinates in the plane (see figure 7*a*) and C is a constant. The exponent α is positive, which ensures that the spiral converges onto the origin (which we have chosen to be the centre of the spiral). We will also calculate the Kolmogorov capacity D'_K of the set of point intersections on the spiral with a straight line cutting through the spiral.

(a) *A cut through the centre of the spiral*

If we choose the line to cut across the centre of the spiral and to be at a given angle Φ with the x axis, then the series of point intersections with the spiral has coordinates (r_n, ϕ_n) that relate to each other by:

$$r_n = C\phi_n^{-\alpha}, \quad (\text{A } 2a)$$

$$\phi_n = \Phi + 2n\pi. \quad (\text{A } 2b)$$

For n large enough ($n \gg \Phi/2\pi$), that series is of the kind

$$r_n \sim n^{-\alpha} \quad (\text{A } 3)$$

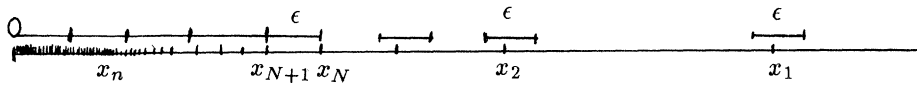


Figure 11. Covering of the set of points $(x_n, 0)$ with boxes of size ϵ . $x_N - x_{N+1}$ is of order ϵ (see (A 5)).

independently of the orientation of the cut, i.e. for any value of Φ between 0 and 2π . The capacity D'_K of the point intersections must therefore also be independent of the orientation of the cut.

In particular, we can choose the cut to be the x axis, in which case $\Phi = 0$ and $r_n = x_n$; (A 3) becomes valid for all $n \geq 1$, and can be written as

$$x_n = C(2\pi n)^{-\alpha}. \tag{A 4}$$

We now estimate the Kolmogorov capacity D'_K of the set of points $(x_n, 0)$, $n = 1, 2, 3, \dots$. Take a small resolution ϵ and compute the smallest integer N for which

$$x_n - x_{n+1} \leq \epsilon \tag{A 5a}$$

for all $n \geq N$. That N is approximately given by:

$$N^{-\alpha} - (N+1)^{-\alpha} \sim \epsilon \tag{A 5b}$$

and as $\epsilon \rightarrow 0$, N becomes so much larger than 1 that we can expand (A 5b) in powers of $1/N$ and obtain at first order:

$$N \sim \epsilon^{-1/(\alpha+1)}. \tag{A 6}$$

In covering the set of points $(x_n, 0)$ with boxes of side-length ϵ , we notice (see figure 11) that one box is needed specifically to cover each point $(x_n, 0)$ for $1 \leq n \leq N$, whereas the remaining $(x_n, 0)$, $n > N$, will all be covered by a total of x_N/ϵ adjacent segments.

It follows therefore, that the number $N(\epsilon)$ of boxes needed to cover the set of point intersections $(x_n, 0)$ is approximately equal to

$$N(\epsilon) \approx N + x_N/\epsilon. \tag{A 7}$$

By using (A 4) and (A 6) we get, as $\epsilon \rightarrow 0$,

$$N(\epsilon) \sim \epsilon^{-1/(\alpha+1)}. \tag{A 8}$$

Comparing (A 8) with (2.1), and assuming that $N(\epsilon)$ is indeed the minimum number of boxes needed to cover the set of points $(x_n, 0)$ as $\epsilon \rightarrow 0$ (we did not prove here that it is the minimum), we obtain the result

$$D'_K = 1/(\alpha + 1). \tag{A 9}$$

(b) *A cut at a distance from the centre*

We chose the cut to be parallel to and at a distance y_c from the x axis. The x coordinates ξ_n of the point intersections of the spiral with that cut are such that

$$\xi_n^2 + y_c^2 = r^2(2\pi n + \delta\phi_n), \tag{A 10}$$

where $\delta\phi_n$ is an angle defined by $\tan \delta\phi_n = y_c/\xi_n$ and $0 \leq \delta\phi_n \leq \frac{1}{2}\pi$. We assume the spiral has only $N - M$ turns; i.e. the x coordinates x_n of the point intersections of the spiral with the x axis are defined for $M \leq n \leq N$, and so are the coordinates ξ_n . x_n is given by (A 4).

We are free to choose the value of M as we please, and so we chose it large enough in order to have $\delta\phi_n \ll 2\pi n$ for all n , and (use (A 1))

$$y_c^2 + \xi_n^2 \approx x_n^2. \tag{A 11}$$

That implies that for values of n such that $x_n \gg y_c$, ξ_n is well approximated by x_n , and therefore the capacity D'_K of the set of point intersections on that cut is also given by (A 9). The difference is that the range of length scales or the number of turns over which (A 9) is now valid is smaller and decreases as y_c increases. Indeed, (A 11) is valid for $n \gg M'$, where $M' = M$ if $y_c \ll x_M$, but is otherwise given by $x_{M'} \sim y_c$. In other words,

$$M' \sim \max \{M, (1/2\pi) (y_c/C)^{-1/\alpha}\}, \tag{A 12a}$$

and (A 9) is valid down to a length scale $\epsilon_{\min} \sim \xi_{M'-1} - \xi_{M'}$ given by

$$\epsilon_{\min} \sim \alpha/M'^{\alpha+1}. \tag{A 12b}$$

(c) *Covering the entire spiral*

We now calculate the Kolmogorov capacity of the entire spiral by considering coverings of the arc itself on the plane, with boxes of size ϵ . We distinguish between two regions of the spiral; the outer coils where, for any $\phi \geq \phi_0$ (ϕ_0 is the starting angle on the spiral),

$$r(\phi) - r(\phi + 2\pi) > \epsilon, \tag{A 13a}$$

and the inner coils where the angles ϕ are so large that (A 13a) does not hold. The critical angle ϕ_ϵ demarcating these two regions is of course such that

$$r(\phi_\epsilon) - r(\phi_\epsilon + 2\pi) = \epsilon \tag{A 13b}$$

and equal to

$$\phi_\epsilon \approx (\epsilon/2\pi\alpha C)^{-1/(1+\alpha)}, \tag{A 14}$$

provided ϕ_ϵ is large enough compared with 2π , which only means that the resolution ϵ should be small enough. If $L(\phi_\epsilon)$ is the total length of the outer coils of the spiral, i.e.

$$L(\phi_\epsilon) = C \int_{\phi_0}^{\phi_\epsilon} \phi^{-\alpha} \sqrt{1 + (\alpha/\phi)^2} d\phi, \tag{A 15}$$

and if $A(\phi_\epsilon)$ is the area of the core containing all the inner coils of the spiral, i.e.

$$A(\phi_\epsilon) \approx \pi r^2(\phi_\epsilon), \tag{A 16}$$

then the minimum number of boxes needed to cover the outer coils is of order $L(\phi_\epsilon)/\epsilon$ and the minimum number of boxes needed to cover the inner coils is of order $A(\phi_\epsilon)/\epsilon^2$. In total, the minimum number of boxes needed to cover the entire spiral is given by

$$N(\epsilon) \sim L(\phi_\epsilon)/\epsilon + A(\phi_\epsilon)/\epsilon^2. \tag{A 17}$$

The Kolmogorov capacity is defined for $\epsilon \rightarrow 0$, but in reality a spiral never has an infinite number of turns, which means that strictly speaking the Kolmogorov capacity of a real spiral (as is found in nature and in numerical simulations) is equal to 1. But for experimental purposes the limit $\epsilon \rightarrow 0$ should be reinterpreted as meaning $\epsilon \ll r(\phi_0)$ or even $\epsilon \leq r(\phi_0) - r(\phi_0 + 2\pi)$ provided that ϵ is kept larger than the smallest distance between two successive coils of the empirical spiral.

We now show that the value of a spiral's D_K is different when the spiral has many turns and when it has only a few. That is equivalent to saying that there are two

ranges of ϵ with two different values of D_K : a range of very small ϵ where many turns of the spiral are resolved, i.e. $\phi_\epsilon - \phi_0 \gg \phi_0$; and a range of ϵ where only a few turns of the spiral are resolved. ϕ_0 can be chosen arbitrarily, so if we chose it to be very large then the previous range is given by $\phi_\epsilon - \phi_0 \ll \phi_0$ and (A 15) can be well approximated as

$$L(\phi_\epsilon) \approx C \int_{\phi_0}^{\phi_\epsilon} \phi^{-\alpha} d\phi. \quad (\text{A } 18)$$

Clearly, the box-counting algorithm applied on a spiral with only a few number of turns will only detect the higher range of ϵ and measure one value of D_K whereas the same algorithm applied to the same spiral with a much larger number of turns will also detect the lower range of ϵ , where D_K takes a different value.

(i) *The case of a large number of resolved turns*

In this case $\phi_\epsilon \gg \phi_0$, and a straightforward integration of (A 18) gives

$$L(\phi_\epsilon) \approx C\phi_\epsilon^{1-\alpha}/(1-\alpha), \quad (\text{A } 19a)$$

if $\alpha < 1$, and

$$L(\phi_\epsilon) \approx C\phi_0^{1-\alpha}/(\alpha-1), \quad (\text{A } 19b)$$

if $\alpha > 1$. Making use of (A 14), we find that the number of boxes needed to cover the outer coils of the spiral scales as

$$L(\phi_\epsilon)/\epsilon \sim \epsilon^{-2/(1+\alpha)}, \quad (\text{A } 20a)$$

when $\alpha < 1$, and as

$$L(\phi_\epsilon)/\epsilon \sim \epsilon^{-1}, \quad (\text{A } 20b)$$

when $\alpha > 1$. The number of boxes needed to cover the inner coils is

$$A(\phi_\epsilon)/\epsilon^2 \sim \epsilon^{-2/(1+\alpha)} \quad (\text{A } 21)$$

and from (2.1) and (A 17) it follows that

$$D_K = \max\{1, 2/(1+\alpha)\}. \quad (\text{A } 22)$$

Equation (A 22) has already been derived by Dupain *et al.* (1983), Gilbert (1988*b*), A. A. Kerstein (personal communication), M. Borgas (personal communication), J. Jiménez (personal communication) and P. Dimotakis (personal communication). It coincides with the asymptotic value of D_K for $\epsilon \rightarrow 0$.

An interesting remark can be drawn from (A 20*b*) and (A 9); when $\alpha > 1$, the spiral has a finite length even though $D'_K > 0$!

(ii) *The case of a small number of resolved turns*

In this case $\phi_\epsilon - \phi_0 \ll \phi_0$. A direct integration and first order expansion of (A 18) gives

$$L(\phi_\epsilon) \approx C(\phi_\epsilon - \phi_0)\phi_0^{-\alpha}. \quad (\text{A } 23)$$

By using (A 14) we can deduce the number of boxes needed to cover the outer coils of the spiral, i.e.

$$L(\phi_\epsilon)/\epsilon \sim \epsilon^{-1/(1+\alpha)}. \quad (\text{A } 24)$$

The number of boxes covering the inner core of the spiral is still given by (A 21) and is negligible compared to (A 24). From (2.1) and (A 17) we can therefore deduce that

$$D_K = 1 + 1/(1+\alpha), \quad (\text{A } 25)$$

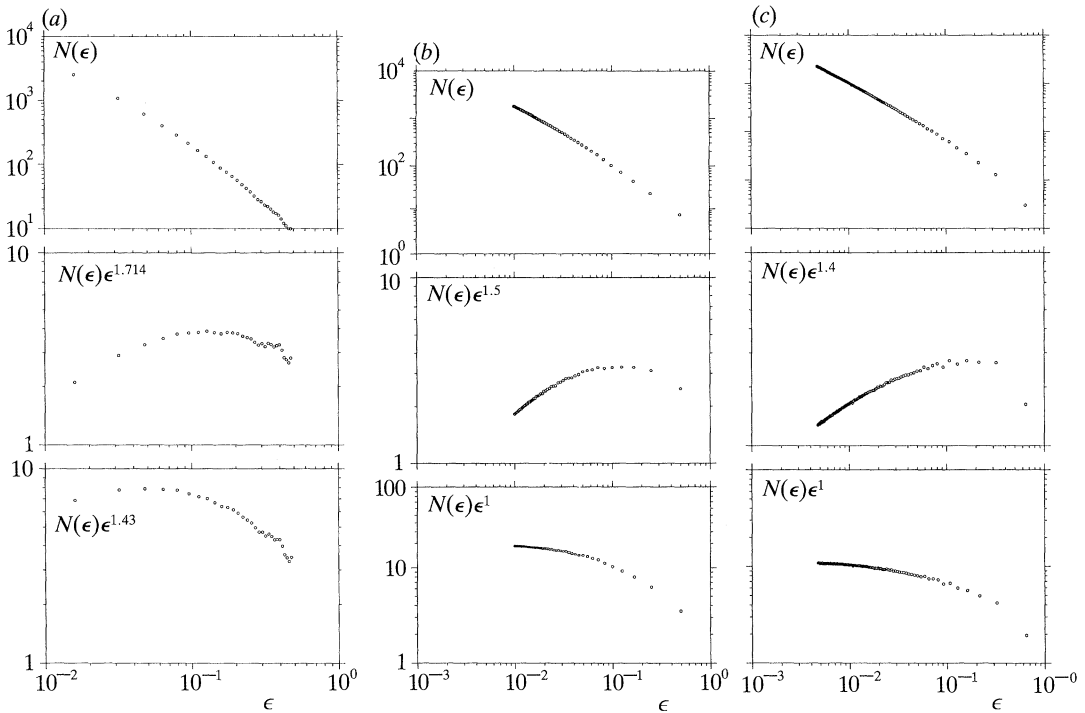


Figure 12. Three log–log plots illustrating the application of the box counting algorithm to spirals with 10 turns. The upper one is of $N(\epsilon)$ against ϵ ; the middle one is of $N(\epsilon)\epsilon^{D_K}$ against ϵ where D_K is calculated as in (A 25). The lower one is the same as the middle one but D_K is calculated on the basis of (A 22). (a) $\alpha = 0.4$; $D_K = 1.714$ on the first three outer turns of the spiral, and $D_K = 1.43$ on the inner turns of the spiral. (b) $\alpha = 1.0$; $D_K = 1.5$ on the first five outer turns of the spiral, and $D_K = 1.0$ on the inner turns of the spiral. (c) $\alpha = 1.5$; $D_K = 1.4$ on the first four outer turns of the spiral, and $D_K = 1.0$ on the inner turns of the spiral.

which is valid when the spiral has only a few turns, or when ϵ is large enough to only resolve a few turns. Note, in particular, that in this limited range of ϵ ,

$$D_K = D'_K + 1. \tag{A 26a}$$

For an interface of topological dimension $E > 1$ rolled up in the form of a spiralling cylindrical structure the previous formula can obviously be generalized;

$$D_K = D'_K + E. \tag{A 26b}$$

We find numerically that (A 25) and (A 26) are valid up to approximately five turns. (A 22) becomes valid when ϵ is small enough to resolve at least seven turns of the spiral. That is indeed the case for $\alpha = 1$ (see figure 12b), and as α grows beyond 1 or tends to 0, (A 25) and (A 26) are found to be valid up to a lesser number of turns (two turns for $\alpha = 0.2$ and two to three turns for $\alpha = 3$). Figure 12a shows log–log plots of $N(\epsilon)$ against ϵ for $\alpha = 0.4$ (where the validity of (A 25) and (A 26) is limited to three turns), and figure 12c shows the same plots for $\alpha = 1.5$ (where the validity of (A 25) and (A 26) is limited to four turns).

It is interesting to note, in conclusion, that the number of boxes of size ϵ needed to cover a logarithmic spiral (i.e. a spiral that is defined by $r(\phi) = \text{const.} \cdot e^{-\phi}$), does not

have a power law dependence on ϵ . If one repeats the previous argument for the set of point intersections of a spiral with a line cutting through its centre, one will find that as $\epsilon \rightarrow 0$,

$$N(\epsilon) \sim \ln(1/\epsilon). \quad (\text{A } 27)$$

The logarithmic spiral is therefore not a K-fractal. One should not think that all accumulation patterns have K-fractal properties. The accumulation has to be slow enough (the logarithmic spiral's convergence onto its centre is too fast) for the pattern, or in particular the spiral, to be locally self-similar.

References

- Batchelor, G. K. 1952 The effect of homogeneous turbulence on material lines and surfaces. *Proc. R. Soc. Lond. A* **213**, 349.
- Batchelor, G. K. 1953 *The theory of homogeneous turbulence*. Cambridge University Press.
- Batchelor, G. K. 1959 Small-scale variation of convected quantities like temperature in turbulent fluid. Part 1. General discussion and the case of small conductivity. *J. Fluid Mech.* **5**, 113.
- Batchelor, G. K. 1969 Computation of the energy spectrum in homogeneous two-dimensional turbulence. *Phys. Fluids Suppl.* II, 233.
- Batchelor, G. K., Howells, I. D. & Townsend, A. A. 1959 Small-scale variation of convected quantities like temperature in turbulent fluid. Part 2. The case of large conductivity. *J. Fluid Mech.* **5**, 134.
- Bedford, T. & Urbanski, M. 1989 The box and Hausdorff dimension of self-affine sets. Faculty of Mathematics and Informatics, Delft University of Technology, The Netherlands. (Preprint.)
- Bracewell, R. N. 1986 *The Fourier transform and its applications*. McGraw-Hill.
- Brachet, M. E., Meneguzzi, M. & Sulem, P. L. 1986 Small scale dynamics of high Reynolds number two-dimensional decaying turbulence. *Phys. Rev. Lett.* **57**, 683.
- Chaté, H. 1987 A very simple model for turbulent flame fronts. Department of Engineering, University of Cambridge, U.K. (Preprint.)
- Dimotakis, P., Lye, R. C. & Papantoniou, D. Z. 1981 In *Proc. 15th Int. Symp. on Fluid Dynamics*. Jachranka, Poland.
- Dupain, Y., Mendes France, M. & Tricot, C. 1983 Dimensions des Spirales. *Bull. Soc. Math. Fr.* **111**, 193.
- Falconer, K. J. 1985 *The geometry of fractal sets*. Cambridge University Press.
- Falconer, K. J. 1988 The Hausdorff dimension of self-affine fractals. *Math. Proc. Camb. Phil. Soc.* **103**, 339.
- Farmer, J. D., Ott, E. & Yorke, J. A. 1983 The dimension of chaotic attractors. *Physica D* **7**, 153.
- Franke, C. & Peters, N. 1985 Untersuchung der Flammenkontur in einer Stark Turbulenten, Vorgemischten Anströmung. In *Proc. Kolloquium des SFB 224 'Motorische Verbrennung'* (ed. F. Pischinger), p. 64. RWTH Aachen.
- Frisch, U. & Orsag, S. A. 1990 Turbulence: challenges for theory and experiment. *Physics Today*, January 1990, p. 24.
- Gibson, M. M. 1963 Spectra of turbulence in a round jet. *J. Fluid Mech.* **15**, 161.
- Gilbert, A. D. 1988a Spiral singularities and spectra in two-dimensional turbulence. *J. Fluid Mech.* **193**, 475.
- Gilbert, A. D. 1988b Ph.D. thesis, University of Cambridge, U.K.
- Gouldin, F. V. 1987 An application of fractals to modelling premixed turbulent flames. *Combust. Flame* **68**, 249.
- Grossman, A. & Morlet, J. 1984 Decomposition of Hardy functions into square integrable wavelets of constant shape. *SIAM J. Math. Anal.* **15**, 723.
- Hausdorff, F. 1919 Dimension and Ausseres Mass. *Math. Annln* **79**, 157.
- Hentschel, H. G. E. & Procaccia, I. 1984 Relative diffusion in turbulent media: the fractal dimension of clouds. *Phys. Rev. A* **29**, 1461.

- Jiménez, J. & Martel, C. 1991 Fractal properties of interfaces in two-dimensional shear-layers. *Phys. Fluids A* **3**, 5.
- Kida, S. 1985 Numerical simulation of two-dimensional turbulence with high symmetry. *J. Phys. Soc. Japan* **54**, 2840.
- Kingdon, R. D. 1987 Ph.D. Thesis. University of Cambridge, U.K.
- Kolmogorov, A. N. 1958 A new invariant for transitive dynamical systems. *Dokl. Akad. Nauk SSSR* **119**, 861.
- Kraichnan, R. H. 1967 Inertial range in two-dimensional turbulence. *Phys. Fluids* **10**, 1417.
- Kraichnan, R. H. & Montgomery, D. 1980 Two-dimensional turbulence. *Rep. Prog. Phys.* **43**, 547.
- Lovejoy, S. 1982 Area-perimeter relation for rain and cloud areas. *Sci. Wash.* **216**, 185.
- Mandelbrot, B. B. 1967 How long is the coast of Britain? Statistical self-similarity and fractional dimension. *Sci. Wash.* **155**, 636.
- Mandelbrot, B. B. 1974 Intermittent turbulence in self-similar cascades: divergence of high moments and dimension of the carrier. *J. Fluid Mech.* **62**, 331.
- Mandelbrot, B. B. 1975 On the geometry of homogeneous turbulence with stress on the fractional dimension of the iso-surfaces of scalars. *J. Fluid Mech.* **72**, 401.
- Mandelbrot, B. B. 1982 The fractal geometry of nature. New York: W. H. Freeman.
- Mantzaras, J., Felton, P. G. & Bracco, F. V. 1989 Is a laminar flame front a passive scalar surface of the turbulent field? In *Int. Proc. Workshop on Physics of Compressible Turbulent Mixing*. Princeton.
- Moffatt, H. K. 1984 Simple Topological Aspects of Turbulent Velocity Dynamics. In *Proc. IUTAM Symp. on Turbulence and Chaotic Phenomena in Fluids* (ed. T. Tatsumi), p. 223. Elsevier.
- North, G. C. & Santavicca, D. A. 1991 The fractal nature of premixed flames. *Combust. Sci. Technol.* (In the press.)
- Orey, S. 1970 Gaussian sample functions and the Hausdorff dimension of level crossings. *Z. Wahrscheinlichkeitstheorie verw. Geb.* **15**, 249.
- Peters, N. 1988 Laminar flamelet concepts in turbulent combustion. In *Proc. 21st Symp. (Int.) on Combustion*, p. 1231. Pittsburgh: The Combustion Institute.
- Phillips, O. M. 1985 Spectral and statistical properties of the equilibrium range in wind-generated gravity waves. *J. Fluid Mech.* **156**, 505.
- Prasad, R. R. & Sreenivasan, K. R. 1989 Quantitative three-dimensional imaging and the structure of passive scalar fields in fully turbulent flows. Mason Laboratory, Yale University, U.S.A. (Preprint.)
- Redondo, J. M. & Linden, P. F. 1988 The fractal dimension of stratified turbulence. Department of Applied Mathematics and Theoretical Physics, University of Cambridge, U.K. (Preprint.)
- Ruelle, D. 1989 *Chaotic evolution and strange attractors*. Cambridge University Press.
- Saffman, P. G. 1968 Lectures on homogeneous turbulence. In *Topics in nonlinear physics* (ed. N. J. Zabusky). Berlin, Heidelberg: Springer-Verlag.
- Saffman, P. G. 1971 On the spectrum and decay of random two-dimensional vorticity distributions at large Reynolds number. *Stud. Appl. Math.* **50**, 377.
- Sreenivasan, K. R. & Meneveau, C. 1986 The fractal facets of turbulence. *J. Fluid Mech.* **173**, 357.
- Sreenivasan, K. R., Ramshankar, R. & Meneveau, C. 1989 Mixing, entrainment and fractal dimensions of surfaces in turbulent flows. *Proc. R. Soc. Lond.* **A 421**, 79.
- Taylor, S. J. 1954 The α -dimensional measure of the graph and set of zones of a brownian path. *Proc. Camb. Phil. Soc.* **51**, Part II, 265.
- Vassilicos, J. C. 1989 On the geometry of lines in two-dimensional turbulence. In *Advances in turbulence 2* (ed. H.-H. Fernholz & H. E. Fiedler). Berlin, Heidelberg: Springer-Verlag.
- Voss, R. F. 1988 Fractals in nature: from characterization to simulation. In *The science of fractal images* (ed. H.-O. Peitgen & D. Saupe). Berlin, Heidelberg: Springer-Verlag.

Received 16 January 1991; accepted 23 April 1991